Ab initio approach to reconstructions of the InP(111)*A* surface: Role of hydrogen atoms passivating surface dangling bonds

Toru Akiyama,* Tomoyuki Kondo, Hiroaki Tatematsu, Kohji Nakamura, and Tomonori Ito
Department of Physics Engineering, Mie University, 1577 Kurima-Machiya, Tsu 514-8507, Japan
(Received 7 October 2008; revised manuscript received 22 October 2008; published 18 November 2008)

The reconstructions on InP(111)*A* surface are systematically investigated using an *ab inito*–based approach, which incorporates chemical potentials in the gas phase of P_2 and H_2 molecules as functions of temperature and pressure. The calculated surface energy clarifies that the reconstruction depends on both hydrogen and phosphorous chemical potentials. The surface phase diagram as function of temperature and P_2 pressure without taking account of passivating H atoms reveals that the stable region for the (2×2) surface with In vacancy is located beyond 450–680 K depending on the pressure, consistent with the experimentally reported temperature range (~670 K). However, the stable temperature range for the $(\sqrt{3}\times\sqrt{3})R30°$ surface with P trimer (below 290–430 K) is much lower than the experimental results (~530 K). Considering a reconstruction partially passivated by H atoms, the stable region for the surface with P trimer expands toward higher temperature by ~200 K and reasonably agrees with experimentally reported temperature range. Furthermore, comparisons of the calculated scanning tunneling microscopy images for the $(\sqrt{3}\times\sqrt{3})R30°$ surface containing P trimer to the experimental data support the plausibility of the surfaces passivated by H atoms. The results obtained thus suggest a possible explanation for the appearance of the $(\sqrt{3}\times\sqrt{3})R30°$ reconstruction on InP(111)*A* surface.

DOI: 10.1103/PhysRevB.78.205318 PACS number(s): 68.35.bg, 68.43.Bc, 81.05.Ea

I. INTRODUCTION

Polar surfaces in group III-V semiconductors, such as GaAs(111), InAs(111), and InP(111), are of great importance in fabricating optoelectronic devices. It has been suggested that the reconstruction of group III-V semiconductor surface satisfies the electron counting model (ECM) in which all dangling bonds of cations (group III atoms) are unoccupied and those of anions (group V atoms) are occupied by electrons.[1] The reconstructions on GaAs(111) surfaces have been investigated by scanning tunneling microscopy (STM),[2–6] x-ray photoemission spectroscopy (XPS),[6] electron-diffraction techniques,[7,8] and total-energy calculations.[5,9–11] These studies have clarified that the Ga-terminated GaAs(111)*A* surface forms a (2×2) lattice with a Ga vacancy in each unit cell, where the ECM is satisfied. The low-temperature STM observation and theoretical calculations[12] have also confirmed the same atomic configuration on In-terminated InAs(111)$A-(2\times2)$ surface.

In contrast, the reconstructions on In-terminated InP(111)*A* surface are somewhat different from those of GaAs(111)*A* and InAs(111)*A* surfaces. Recent observations using the STM, low-energy electron diffraction (LEED), and XPS have revealed two types of reconstructions on InP(111)*A* surface fabricated by metalorganic vapor-phase epitaxy (MOVPE).[13] The (2×2) reconstruction with In vacancy, as also seen in GaAs(111)*A* and InAs(111)*A* surfaces, has been observed in In-rich condition at temperatures around 400 °C. In P-rich condition around 250 °C, on the other hand, the surface changes into the $(\sqrt{3}\times\sqrt{3})R30°$ ("*R*30°" is omitted hereafter for simplicity) surface and is proposed to form a reconstruction consisting P trimer in every unit cell. Since the ECM is destroyed, this surface is generally unstable against the surfaces satisfying the ECM. Recent total-energy calculations[14] for the (2×2) and $(\sqrt{3}\times\sqrt{3})$ reconstructions with P trimer on InP(111)*A* surface have clarified that the $(\sqrt{3}\times\sqrt{3})$ surface is stable compared to the (2×2) surface and proposed several hydrogen passivated structures satisfying the ECM. However, the relative stability among various reconstructions including the (2×2) surface with In vacancy and their counterparts with H atoms is still unclear. Moreover, total-energy calculations[15] have clarify that hydrogen atoms crucially affect the reconstruction of InP(001) surfaces exhibiting the (2×1) reconstruction under the MOVPE and chemical beam epitaxy growth condition, implying that the reconstructions of InP(111)*A* surface under the MOVPE growth are also affected by hydrogen atoms.

In our previous study, we successfully clarified the reconstruction on GaAs(001) and GaAs(111)*B* surfaces using *ab inito*–based approach in which surface phase diagram depending on temperature and pressure is described by comparing the calculated adsorption energy to chemical potential estimated by quantum statistical mechanics.[16–19] In this paper, in order to discuss the structural change depending on surface conditions, we extend the approach to investigate surface phase diagrams on InP(111)*A* surface. Effects of hydrogen passivation on the appearance of the $(\sqrt{3}\times\sqrt{3})$-type reconstruction are examined using the calculated surface diagrams. In order to support the observed STM images, we furthermore simulate the STM images of the stabilized reconstructions and compare them to the experimental data.

II. CALCULATION PROCEDURE

For the reconstructions on the InP(111)*A* surface, we adopt the (2×2) surfaces with P trimer and In vacancy, as shown in Figs. 1(a) and 1(b), respectively. The surface with

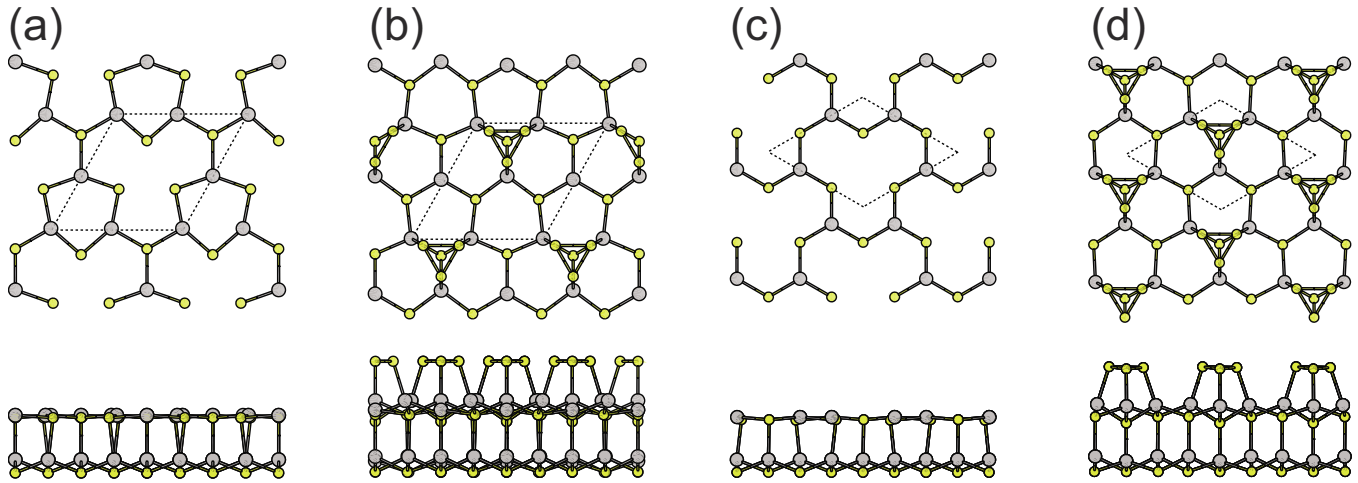

FIG. 1. (Color online) Top and side views of the geometries of the (2×2) surfaces with (a) In vacancy and (b) P trimer and the $(\sqrt{3}\times\sqrt{3})$ surfaces with (c) In vacancy and (d) P trimer. Large and small circles represent In and P atoms, respectively. The unit cell is enclosed by dashed lines.

In vacancy has been already observed on GaAs(111)*A* (Refs. 2–6) and InAs(111)*A* (Ref. 12) surfaces so that this reconstruction is expected to appear on InP(111)*A* surface. It can also be expected that the surface with P trimer appears for P-rich condition because it satisfies the ECM. Indeed, the (2×2) reconstruction with As trimer has been theoretically proposed as a possible reconstruction on GaAs(111)*A* (Refs. 9 and 10) and InAs(111)*A* surfaces.[12] For the reconstructions under hydrogen ambient conditions, the surfaces passivated by H atoms are also adopted. Furthermore, we consider their counterparts for the $(\sqrt{3}\times\sqrt{3})$ surface based on the STM and LEED observations which have reported the $(\sqrt{3}\times\sqrt{3})$ lattice,[13] as shown in Figs. 1(c) and 1(d). Since these reconstructions do not satisfy the ECM, we take account of the surface satisfying the ECM and possessing similar periodicity to the $(\sqrt{3}\times\sqrt{3})$ lattice. As possible reconstructions satisfying the ECM, as shown in Fig. 2, we adopt the $(2\sqrt{3}\times2\sqrt{3})$ surface in which some of P dangling bonds are terminated by H atoms—all the H atoms terminate all of dangling bonds in one of P trimers in Fig. 2(a), whereas each H atom does one dangling bond in three of four P trimers consisting the $(2\sqrt{3}\times2\sqrt{3})$ surface in Fig. 2(b). This kind of hydrogen-terminated surfaces is proved to be realized for the MOVPE-grown InP(001) surface.[15,20,21]

In order to discuss the relative stability among various surface reconstructions, we calculate surface formation energy according to the conventional thermodynamic formalism[11] wherein the difference in energies depends linearly on the chemical potentials of P and H atoms (μ_P and μ_H, respectively). The surface formation energy γ_{surf} is given by

$$\gamma_{surf}(\mu_P,\mu_H) = E_{tot} - \mu_{InP}N_{In} - \mu_P(N_P - N_{In}) - \mu_H N_H, \quad (1)$$

where E_{tot} is the total energy of in InP(111)*A* surface, N_{In} (N_P,N_H) the number of In (P, H) atoms, and μ_{InP} the chemical potential of bulk InP. The zero of μ_H is set to the energy of H_2 molecule $\mu_H(H_2)$. The allowable value for μ_P in this study is

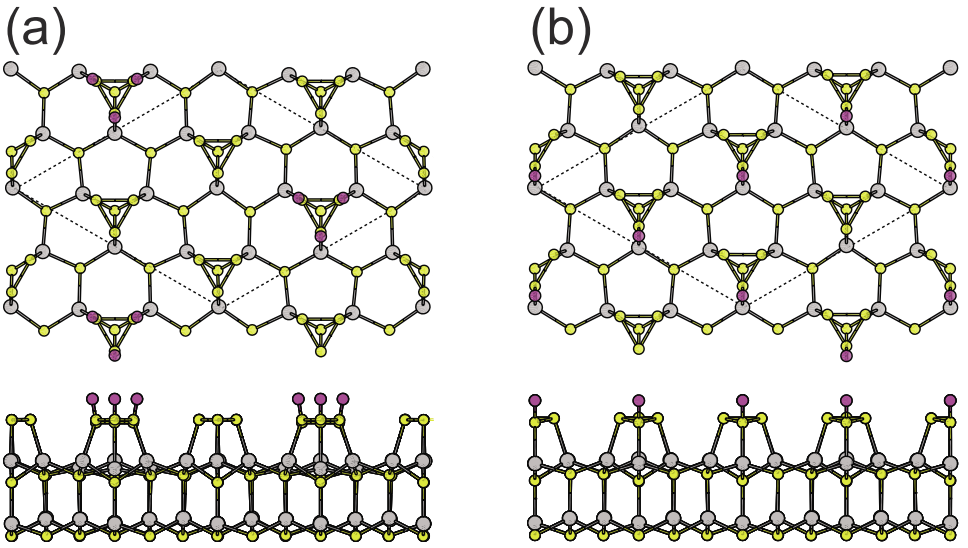

FIG. 2. (Color online) Top and side views of the geometries of the $(2\sqrt{3}\times2\sqrt{3})$ surfaces, where H atoms passivate (a) one and (b) three of four P trimers in the unit cell. Large and small circles represent In and P atoms, respectively. The H atoms passivating dangling bonds are represented by red (filled) circles. The unit cell is enclosed by dashed lines.

$$\mu_{\mathrm{P}}(\mathrm{bulk}) - \Delta H_f < \mu_{\mathrm{P}} < \mu_{\mathrm{P}}(\mathrm{bulk}), \tag{2}$$

where $\mu_{\mathrm{P}}(\mathrm{bulk})$ is the chemical potential of P in the condensed phase and $\Delta H_f[=\mu_{\mathrm{In}}(\mathrm{bulk})+\mu_{\mathrm{P}}(\mathrm{bulk})-\mu_{\mathrm{InP}}]$ the heat of formation. For the bulk calculations, we calculate the energy of In (P) in face-centered tetragonal (orthorhombic) structure and obtain the value of 0.87 eV for ΔH_f.

Furthermore, we apply an *ab inito* approach to study the relative stability among various reconstructions and predict phase diagrams depending on temperature and pressure of molecular species. The phase diagrams are obtained by considering adsorption-desorption behavior of P (H) which can be described by comparing the free energy of ideal gas per one particle (chemical potential) μ_{gas} to the adsorption energy E_{ad}. The chemical potential of molecule is expressed as[22–24]

$$\mu_{\mathrm{gas}} = -k_B T \ln\left(\frac{k_B T}{p} \times g \times \zeta_{\mathrm{trans}} \times \zeta_{\mathrm{rot}} \times \zeta_{\mathrm{vib}}\right), \tag{3}$$

where k_B is Boltzmann's constant, T is the gas temperature, g is the degree of degeneracy of electron energy level, and p is the pressure. ζ_{trans}, ζ_{rot}, and ζ_{vib} are the partition functions for translational, rotational, and vibrational motions, respectively. Details of these partition functions are expressed elsewhere.[22,23] The adsorption energy E_{ad} (per atom) is calculated by the energy difference between two structures using total-energy electronic-structure calculations within the density-functional theory. Relative stability between two structures is determined by comparing μ_{gas} to E_{ad}. That is, the structure corresponding to adsorbed surface is favorable when E_{ad} is less than μ_{gas}, whereas desorbed surface is stabilized when μ_{gas} is less than E_{ad}. We note that the relationship between In chemical potential $\mu_{\mathrm{In}}+\mu_{\mathrm{P}}=\mu_{\mathrm{InP}}$ is applied for the comparison between the surface with P trimer and that with In vacancy.

The total-energy calculations are performed within the generalized gradient approximation (GGA) (Ref. 25) in the density-functional theory. We use norm-conserving pseudopotentials[26] with partial core correction.[27] The conjugate-gradient minimization technique is used for both the electronic-structure calculation and the geometry optimization.[28,29] In the optimized geometries the remaining forces acting on the atoms are less than 5.0×10^{-3} Ry/Å. The valence wave functions are expanded by the plane-wave basis set with a cutoff energy of 12.25 Ry, which gives enough convergence of total energy to discuss the relative stability. We take slab models consisting of eight atomic layers with pseudohydrogen atoms[30] and a vacuum region equivalent to nine atomic layer thickness. The atoms belonging to bottom bilayer are fixed at their ideal positions. The k points which correspond to 32 points in the irreducible part of the (1×1) surface Brillouin zone are used throughout this study.

III. RESULTS AND DISCUSSION

Figure 3 shows the stable reconstructions obtained by the surface energy (per unit area) using Eq. (1). The calculated surface energy demonstrates that the reconstruction depends on the chemical potentials of P and H. The $(\sqrt{3}\times\sqrt{3})$ surface with P trimer and the (2×2) surfaces appear as stable reconstructions for H-free case, while the $(2\sqrt{3}\times2\sqrt{3})$ surface shown in Fig. 2(b) and the (2×2) surface with In vacancy emerge as H-passivated surfaces.

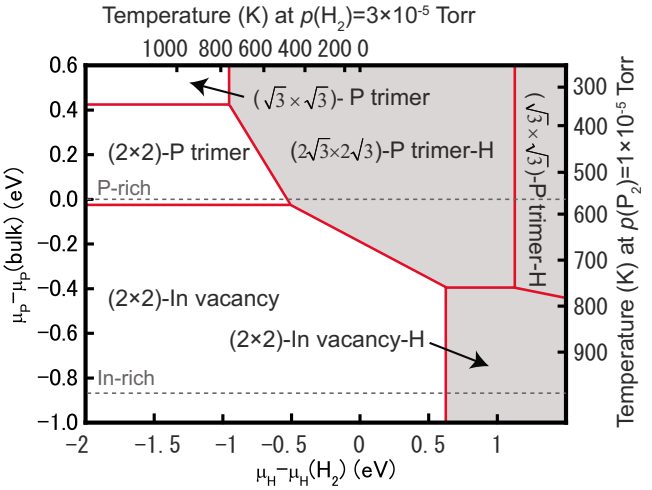

FIG. 3. (Color online) Calculated stable reconstructions as functions of H chemical potential μ_{H} and P chemical potential μ_{P}. Shaded area denotes the stabilized region for H-passivated surface. Dashed lines indicate the approximate range of the thermodynamically allowed values of μ_{P}. The chemical potential of hydrogen is given with respect to that of H_2 molecule. Right (top) axis shows temperature of P_2 (H_2) gas corresponding to pressures at 1×10^{-5} (3×10^{-5}) Torr, which is referred from the experimental condition in Ref. 13.

We find that the ideal $(111)A$ surface, the $(\sqrt{3}\times\sqrt{3})$ surface with In vacancy, and the $(2\sqrt{3}\times2\sqrt{3})$ surface shown in Fig. 2(a) are always metastable over entire chemical-potential range considered in this study. The stable structure for the surfaces without H atom can be interpreted in terms of the deviation from the ECM. The (2×2) surfaces satisfy the ECM and are semiconducting as shown in Figs. 4(a) and 4(b). In contrast, the number of excess electrons [3/4 of an electron per (1×1) unit] is quite large on the ideal $(111)A$ surface. As a result, the surface energy is much higher than the most stable one (by ~25 meV/Å^2). For the $(\sqrt{3}\times\sqrt{3})$ surface with In vacancy, 3/4 of an electron [1/4 of an electron per (1×1) unit] is lacking to satisfy the ECM. The band structure around the Fermi level shown in Fig. 4(c) represents the electron deficit exhibiting metallic character. Due to relatively small number of deficit electrons compared to the ideal $(111)A$ surface, the surface energy is slightly higher than that in the (2×2) surface with In vacancy. The $(\sqrt{3}\times\sqrt{3})$ with P trimer is also lacking by 3/4 of an electron, so that this surface becomes stable only for very P-rich condition as discussed below. As seen in the $(\sqrt{3}\times\sqrt{3})$ with In vacancy, the deficit of electrons can be recognized from the band structure shown in Fig. 4(d), but its electronic structure is slightly different from that in the $(\sqrt{3}\times\sqrt{3})$ with In vacancy. The valence electrons in the $(\sqrt{3}\times\sqrt{3})$ surface with P trimer partially occupy the localized states caused by p orbitals of P trimer normal to the surface, while the delocalized (dispersive) p orbitals of surface P atoms parallel to the

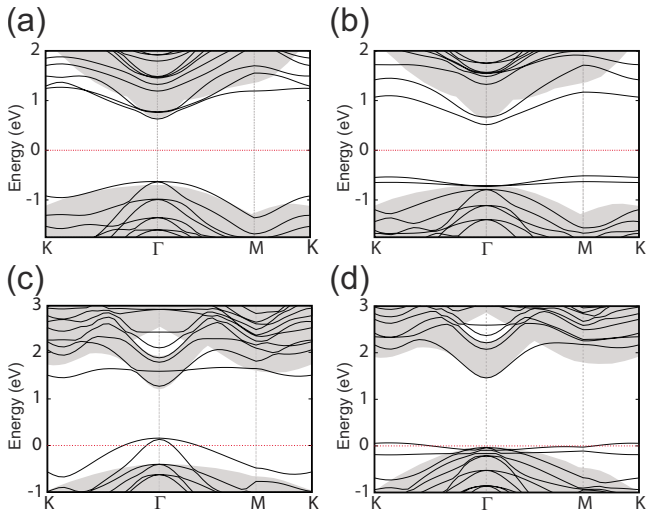

FIG. 4. (Color online) Kohn-Sham band structure of the (2×2) surfaces with (a) In vacancy and (b) P trimer, and the $(\sqrt{3}\times\sqrt{3})$ surfaces with (c) In vacancy and (d) P trimer shown in Figs. 1(a)–1(d), respectively. The origin of energy is set to the Fermi energy. The projected bulk band structure is shown by gray area.

growth direction are partially occupied by electrons in the $(\sqrt{3}\times\sqrt{3})$ surface with In vacancy.

For the surfaces passivated by H atoms, the $(2\sqrt{3}\times2\sqrt{3})$ surface passivating three P trimers [Fig. 2(b)] is stable compared to that passivating one P trimer [Fig. 2(a)] with an energy gain of 1.92 eV, although both surfaces are found to be semiconducting as shown in Fig. 5. We speculate that the repulsive interaction among H atoms is prominent for the surface passivating one P trimer because the distances between H atoms on this surface (~2.69 Å) are much smaller than those on the other surface (~7.17 Å). Our calculations for H-passivated surfaces clarify that under plausible μ_H condition in the MOVPE growth ($\mu_H\sim0$ eV) the $(2\sqrt{3}\times2\sqrt{3})$ surface is stable over wide range of μ_P, indicating that the $(2\sqrt{3}\times2\sqrt{3})$ surface with H atoms is stabilized by satisfying the ECM. Indeed, the adsorption energy of hydrogen in the $(2\sqrt{3}\times2\sqrt{3})$ surface (−0.92 eV) is much smaller than those in the (2×2) surfaces with P trimer and In vacancy (0.32 and 0.62 eV, respectively). Consequently, the stable region for the H-passivated (2×2) surfaces with P trimer is corroded by the $(2\sqrt{3}\times2\sqrt{3})$ surface passivated by H atoms.

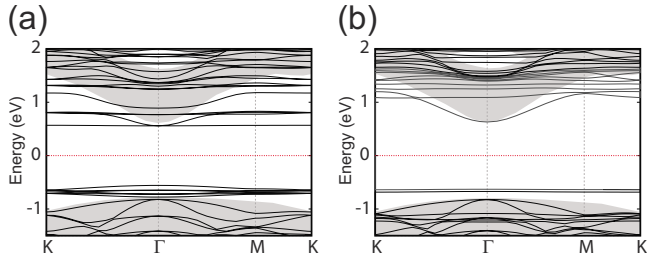

FIG. 5. (Color online) Kohn-Sham band structure of the $(2\sqrt{3}\times2\sqrt{3})$ surfaces, where H atoms passivate (a) one and (b) three of four P trimers in the unit cell, as shown in Figs. 2(a) and 2(b), respectively. The origin of energy is set to the Fermi energy. The projected bulk band structure is shown by gray area.

In the case of $\mu_H-\mu_H(H_2)\ll0$, which corresponds to the molecular-beam epitaxy (MBE) growth condition, the surface forms the reconstructions typical for the clean (111)*A* surface. Trends in the stable structure on InP(111)*A* surface reasonably agree with that in GaAs(111)*A* and InAs(111)*A* surfaces,[11,12] but are different from the results on InP(111)*A* surface in Ref. 14, where the $(\sqrt{3}\times\sqrt{3})$ surface with P trimer is more stable than the (2×2) surface with P trimer over entire μ_P range. Although we are unable to determine the origin of the discrepancy, it might be due to the difference in exchange-correlation functional or treatment of In-4*d* electrons. For In-rich condition $[\mu_P-\mu_P(\text{bulk})\leq-0.02$ eV], the (2×2) surface with In vacancy is stable and the (2×2) surface with P trimer is favorable for P-rich condition. The $(\sqrt{3}\times\sqrt{3})$ surface with P trimer is stable only for very P-rich condition $[\mu_P-\mu_P(\text{bulk})\geq0.42$ eV]. Considering that the energy range of μ_P in which the $(\sqrt{3}\times\sqrt{3})$ surface is stabilized is much higher than the thermodynamically allowed region, it is expected that the clean $(\sqrt{3}\times\sqrt{3})$ reconstruction could not appear under the MBE growth condition.

For $\mu_H-\mu_H(H_2)\geq-0.92$ eV, in contrast, the reconstruction with H atoms appears and the stable region for the $(2\sqrt{3}\times2\sqrt{3})$ surface passivated by H atoms increases with increasing μ_H. This implies that under H-rich condition such as the MOVPE growth the surfaces passivated by H atoms could appear as stable phase. It should be noted that for $\mu_H-\mu_H(H_2)\geq-0.48$ eV the stable region for the (2×2) surface with P trimer disappears and the $(2\sqrt{3}\times2\sqrt{3})$ surface changes directly into the (2×2) surface with In vacancy with decreasing μ_P. Considering the difficulty to detect hydrogen and the possibility for attaching H atoms at P trimers, the $(\sqrt{3}\times\sqrt{3})$ surface observed in the STM and LEED can be regarded as a kind of H-passivated surfaces such as the $(2\sqrt{3}\times2\sqrt{3})$ surface shown in Fig. 2(b). In this case, under H-rich condition InP(111)*A* surface forms the (2×2) reconstruction with In vacancy or the $(\sqrt{3}\times\sqrt{3})$ like surface on which some of P trimers are passivated by H atoms. If we assume that the $(2\sqrt{3}\times2\sqrt{3})$ surface considered in this study is a kind of hydrogen stabilized surface, there appear only two types of reconstructions, qualitatively consistent with experimental results.[13]

In order to clarify the reconstructions more quantitatively, we calculate surface phase diagram as function of temperature and pressure using Eq. (3). Figure 6(a) shows the calculated surface phase diagram corresponding to hydrogen absent condition.[31] The figure demonstrates that the stable region for the (2×2) surface with In vacancy is located beyond 450–680 K depending on the pressure of P_2 molecule. For low P_2 pressure condition, the (2×2) surface is stabilized beyond 500 K, reasonably consistent with the experimental result where the (2×2) surface appears around 670 K in vacuum.[13] Our calculated phase diagram also implies that the $(\sqrt{3}\times\sqrt{3})$ surface with P trimer appears below 290–430 K, but the stable region is much lower than the experimentally reported temperature (520 K) after the exposure of phosphine at 1×10^{-5} Torr. Moreover, the (2×2) surface with P trimer, which appears between the $(\sqrt{3}\times\sqrt{3})$ surface with P trimer and the (2×2) surface with In vacancy in the present study, has never been observed in the experiments.[13] The discrepancy between the calculated surface phase dia-

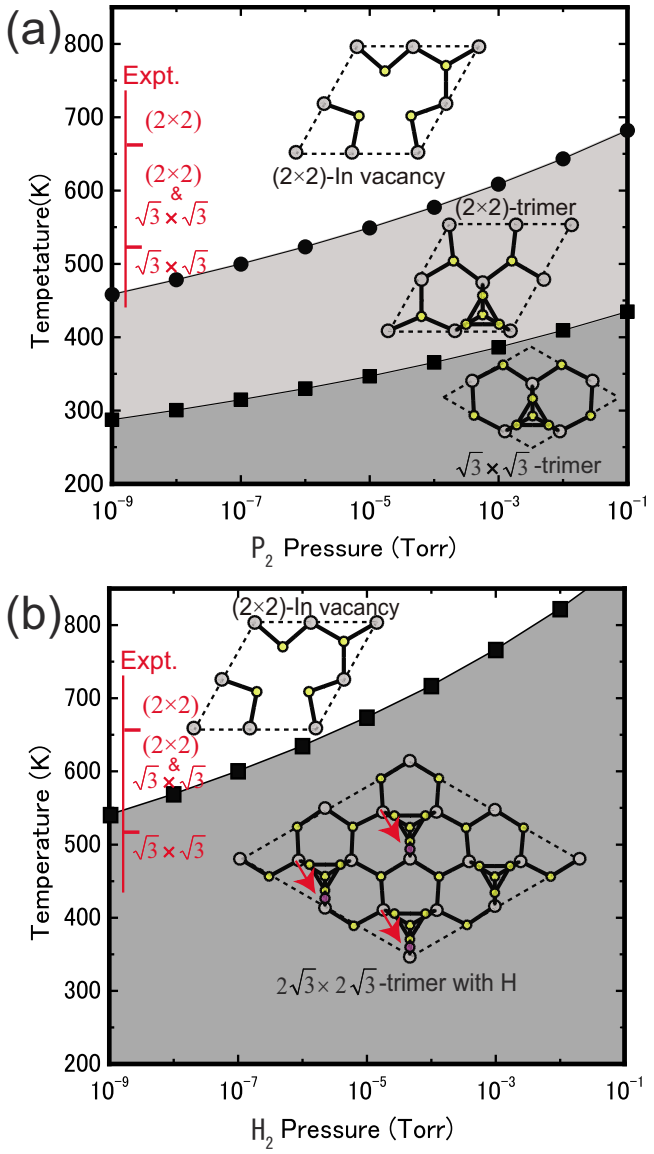

FIG. 6. (Color online) Calculated surface phase diagrams of (a) clean InP(111)*A* surfaces and (b) InP(111)*A* surfaces taking account of H passivation as functions of temperature and pressure, along with their geometries. Experimental temperature ranges (red line) are attached to temperature axis. The positions of H atoms passivating surface dangling bonds are indicated by arrows.

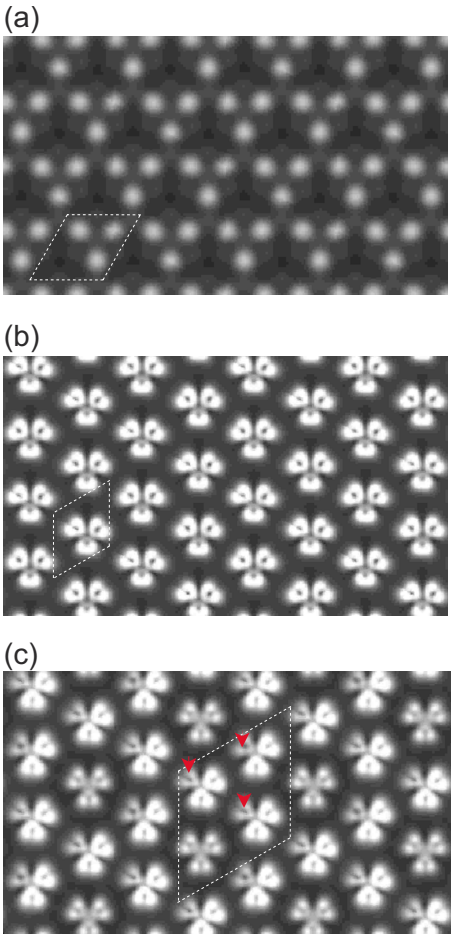

FIG. 7. (Color online) Calculated STM images of (a) the (2×2) surface with In vacancy, (b) the $(\sqrt{3}\times\sqrt{3})$ surface with P trimer, and (c) the $(2\sqrt{3}\times2\sqrt{3})$ surface partially passivated by H atoms. The unit cells are also shown. The positions of H atoms passivating surface dangling bonds are indicated by arrows. A bias voltage of +3 eV is used to allow for a comparison to the experimental data.

gram and the experiment implies that the observation $(\sqrt{3}\times\sqrt{3})$ reconstruction cannot be explained by only considering hydrogen-free InP(111)*A* surface.

Taking account of the presence of H atoms, however, the discrepancy can be resolved. Figure 6(b) shows the calculated surface phase diagram as function of temperature and H_2 pressure. Here, the pressure of P_2 is taken to be one third of H_2 pressure, assuming that most of phosphines around InP(111)*A* surface dissociate and then P_2 and H_2 molecules are present according to the dissociation reaction $2PH_3 \rightarrow P_2+3H_2$. The stable temperature range for the $(2\sqrt{3}\times2\sqrt{3})$ surface with H atoms is found to be ~200 K higher than that for the $(\sqrt{3}\times\sqrt{3})$ surface without H atom. This is because the $(2\sqrt{3}\times2\sqrt{3})$ surface satisfies the ECM and then the E_{ad} of hydrogen (−0.92 eV) in the $(2\sqrt{3}\times2\sqrt{3})$ surface is larger than that of phosphorus in the (2×2) surface with P trimer (−0.53 eV). For H_2 pressure less than 1×10^{-5} Torr, the stable region for the (2×2) surface is located beyond 550–650 K and the $(2\sqrt{3}\times2\sqrt{3})$ surface is stabilized below 550–650 K. These temperature ranges reasonably agree with the experimental observation of the (2×2) and the $(\sqrt{3}\times\sqrt{3})$ surfaces (670 and 520 K, respectively). The phase diagram also indicates that due to the small energy difference between these reconstructions both reconstructions could appear under the conditions corresponding to the phase boundary. Indeed, the phase boundary (550–650 K) coincides with the experimental temperature range for the observation mixture of the $(\sqrt{3}\times\sqrt{3})$ and the (2×2) phases.[13]

Finally, we compare the calculated STM images to the experimental data. Figure 7 displays the calculated STM images for the stable surfaces according to the Tersoff-Hamann approach.[32] A bias voltage of 3 eV is used to allow for a comparison to the experimental data. As for the (2×2) surface with In vacancy shown in Fig. 7(a), the bright spots are

due to the unoccupied p orbitals of surface In atoms, as indicated by the STM observation for empty electronic states on InAs(111)A surface.[12] Although the resolution of the observed STM image for the empty states is not high enough to clearly resolve the bright and dark spots, the bright spots in the unit cell in Fig. 7(a) reasonably agree with the experimental data.[13]

As shown in Figs. 7(b) and 7(c), there is no significant difference between their bright positions for the calculated STM images of the $(\sqrt{3}\times\sqrt{3})$ and $(2\sqrt{3}\times 2\sqrt{3})$ surfaces. This is because the antibonding states of P-P bonds which mainly contribute the bright spots of the STM images are not affected significantly by hydrogen passivation. Although the bright regions of P atoms passivated H atoms [arrows in Fig. 7(c)] and those of the remaining pristine P trimer on the $(2\sqrt{3}\times 2\sqrt{3})$ surface are slightly weak compared to those on the $(\sqrt{3}\times\sqrt{3})$ surface, such an obscure difference might be beyond the resolution of experimental STM images. If we combine all bright spots of each P trimer together, the size of combined bright region in both the $(\sqrt{3}\times\sqrt{3})$ and $(2\sqrt{3}\times 2\sqrt{3})$ surfaces agrees well with that in the experiment.[13] This implies that even if some of P trimers are passivated by H atoms overall image of the surfaces is similar to that of the $(\sqrt{3}\times\sqrt{3})$ surface. The calculated STM images thus support the presence of the surfaces with P trimer partially terminated by H atoms.

IV. SUMMARY

We have systematically investigated the reconstructions on InP(111)A surface using *ab inito*–based approach. We have found that the stable reconstruction depends on the chemical potentials of P and H—the (2×2) reconstruction with In vacancy is stable for In-rich condition while the $(\sqrt{3}\times\sqrt{3})$ reconstruction with an P trimer is favorable for very P-rich condition. The (2×2) surface with P trimer is stabilized between the (2×2) surface with In vacancy and the $(\sqrt{3}\times\sqrt{3})$ surface with P trimer. The surface phase diagram as functions of temperature and P_2 pressure also demonstrates that the stable region for the (2×2) surface with In vacancy is located beyond 450–680 K depending on the pressure, consistent with the experimentally reported temperature range (~670 K). However, the stable region for the $(\sqrt{3}\times\sqrt{3})$ surface with P trimer (below 290–430 K) is much lower than the experimental results (~530 K). Taking account of a reconstruction partially passivated by H atoms, the stable region for the surface with P trimer expands toward higher temperature by 200 K and reasonably agrees with experimentally reported temperature range for the $(\sqrt{3}\times\sqrt{3})$ fabricated by metal organic vapor-phase epitaxy. Moreover, our comparisons of the calculated STM images for the surfaces containing P trimer to the experimental data support the plausibility of the surface passivated by H atoms. These results suggest a possible explanation for the appearance of the $(\sqrt{3}\times\sqrt{3})$ reconstruction with P trimer on InP(111)A surface.

ACKNOWLEDGMENTS

This work was supported in part by Grant-in-Aid for Scientific Research from JSPS under Contract No. 18560020. Codes used in this work are based on Tokyo *Ab-initio* Program Package (TAPP). Computations were performed at RCCS (National Institutes of Natural Sciences) and ISSP (University of Tokyo).

*akiyama@phen.mie-u.ac.jp

[1] M. D. Pashley, Phys. Rev. B **40**, 10481 (1989).
[2] D. K. Biegelsen, R. D. Bringans, J. E. Northrup, and L. E. Swartz, Phys. Rev. Lett. **65**, 452 (1990).
[3] K. W. Haberern and M. D. Pashley, Phys. Rev. B **41**, 3226 (1990).
[4] J. M. C. Thornton, D. A. Woolf, and P. Weightman, Surf. Sci. **380**, 548 (1997).
[5] A. Ohtake, J. Nakamura, T. Komura, T. Hanada, T. Yao, H. Kuramochi, and M. Ozeki, Phys. Rev. B **64**, 045318 (2001).
[6] J. M. C. Thornton, P. Weightman, D. A. Woolf, and C. J. Dunscombe, Phys. Rev. B **51**, 14459 (1995).
[7] S. Y. Tong, G. Xu, and W. N. Mei, Phys. Rev. Lett. **52**, 1693 (1984).
[8] J. Bohr, R. Feidenhansl, M. Nielsen, M. Toney, R. L. Johnson, and I. K. Robinson, Phys. Rev. Lett. **54**, 1275 (1985).
[9] E. Kaxiras, Y. Bar-Yam, J. D. Joannopoulos, and K. C. Pandey, Phys. Rev. B **35**, 9625 (1987).
[10] E. Kaxiras, Y. Bar-Yam, J. D. Joannopoulos, and K. C. Pandey, Phys. Rev. B **35**, 9636 (1987).
[11] N. Moll, A. Kley, E. Pehlke, and M. Scheffler, Phys. Rev. B **54**, 8844 (1996).
[12] A. Taguchi and K. Kanisawa, Appl. Surf. Sci. **252**, 5263 (2006).
[13] C. H. Li, Y. Sun, D. C. Law, S. B. Visbeck, and R. F. Hicks, Phys. Rev. B **68**, 085320 (2003).
[14] K. Chuasiripattana and G. P. Srivastava, Appl. Surf. Sci. **252**, 7678 (2006).
[15] W. G. Schmidt, P. H. Hahn, F. Bechstedt, N. Esser, P. Vogt, A. Wange, and W. Richter, Phys. Rev. Lett. **90**, 126101 (2003).
[16] T. Ito, K. Tsutsumida, K. Nakamura, Y. Kangawa, K. Shiraishi, A. Taguchi, and H. Kageshima, Appl. Surf. Sci. **237**, 194 (2004).
[17] H. Ishizaki, T. Akiyama, K. Nakamura, K. Shiraishi, A. Taguchi, and T. Ito, Appl. Surf. Sci. **244**, 186 (2005).
[18] T. Ito, T. Akiyama, and K. Nakamura, Appl. Surf. Sci. **254**, 7663 (2008).
[19] H. Tatematsu, K. Sano, T. Akiyama, K. Nakamura, and T. Ito, Phys. Rev. B **77**, 233306 (2008).
[20] L. Li, B. K. Han, Q. Fu, and R. F. Hicks, Phys. Rev. Lett. **82**, 1879 (1999).
[21] Q. Fu, E. Negro, G. Chen, D. C. Law, C. H. Li, R. F. Hicks, and K. Raghavachari, Phys. Rev. B **65**, 075318 (2002).
[22] Y. Kangawa, T. Ito, A. Taguchi, K. Shiraishi, and T. Ohachi, Surf. Sci. **493**, 178 (2001).
[23] Y. Kangawa, T. Ito, Y. S. Hiraoka, A. Taguchi, K. Shiraishi, and T. Ohachi, Surf. Sci. **507-510**, 285 (2002).

[24] C. G. Van de Walle and J. Neugebauer, Phys. Rev. Lett. **88**, 066103 (2002).
[25] J. P. Perdew, K. Burke, and M. Ernzerhof, Phys. Rev. Lett. **77**, 3865 (1996).
[26] N. Troullier and J. L. Martins, Phys. Rev. B **43**, 1993 (1991).
[27] S. G. Louie, S. Froyen, and M. L. Cohen, Phys. Rev. B **26**, 1738 (1982).
[28] J. Yamauchi, M. Tsukada, S. Watanabe, and O. Sugino, Phys. Rev. B **54**, 5586 (1996).
[29] H. Kageshima and K. Shiraishi, Phys. Rev. B **56**, 14985 (1997).
[30] K. Shiraishi, J. Phys. Soc. Jpn. **59**, 3455 (1990).
[31] The stable structure depending on temperature at P_2 pressure of 1.0×10^{-5} Torr can also be seen from temperature (right) axis in Fig. 3.
[32] J. Tersoff and D. R. Hamann, Phys. Rev. B **31**, 805 (1985).